Journal of Luminescence 170 (2016) 161–167

Contents lists available at ScienceDirect

Journal of Luminescence

journal homepage: www.elsevier.com/locate/jlumin

Full Length Article

Intrinsic and defect related luminescence in double oxide films of Al–Hf–O system under soft X-ray and VUV excitation

V.A. Pustovarov [a,*], T.P. Smirnova [b], M.S. Lebedev [b], V.A. Gritsenko [c,d], M. Kirm [e]

[a] Ural Federal University, 19 Mira Street, 620002 Yekaterinburg, Russia
[b] Nikolaev Institute of Inorganic Chemistry, Siberian Branch of Russian Academy of Science, Novosibirsk 630090 Russia
[c] Institute of Semiconductor Physics, Siberian Branch of Russian Academy of Sciences, Novosibirsk 630090 Russia
[d] Novosibirsk National Research University, 2 Pirogova Street, 630090 Novosibirsk, Russia
[e] Institute of Physics, University of Tartu, 14c Ravila, 50411 Tartu, Estonia

ARTICLE INFO

Article history:
Received 3 June 2015
Received in revised form
18 October 2015
Accepted 21 October 2015
Available online 30 October 2015

Keywords:
Time-resolved luminescence
Thin films
Hafnia
Alumina
Self-trapped exciton
Defects

ABSTRACT

Low temperature time-resolved luminescence spectra in the region of 2.5–9.5 eV under soft X-ray excitation as well as time-resolved luminescence excitation spectra in the UV–VUV region (3.7–12 eV) of solid solutions $Al_xHf_yO_{1-x-y}$ thin films were investigated. The values of x and Al/Hf ratio were determined from X-ray photoelectron srectroscopy data. Hafnia films and films mixed with alumina were grown in a flow-type chemical vapor deposition reactor with argon as a carrier gas. In addition, pure alumina films were prepared by the atomic layer deposition method. A strong emission band with the peak position at 4.4 eV and with the decay time in the μs-range was revealed for pure hafnia films. The emission peak at 7.74 eV with short nanosecond decay kinetics was observed in the luminescence spectra for pure alumina films. These emission bands were ascribed to the radiative decay of self-trapped excitons (an intrinsic luminescence) in pure HfO_2 and Al_2O_3 films, respectively. Along with intrinsic host emission, defect related luminescence bands with a larger Stokes shift were observed. In the emission spectra of the solid solution films (x=4; 17; 20 at%) the intrinsic emission bands are quenched and only the luminescence of defects (an anion vacancies) was observed. Based on transformation of the luminescence spectra and ns-luminescence decay kinetics, as well as changes in the time-resolved luminescence and luminescence excitation spectra, the relaxation processes in the films of solid solution are discussed.

© 2015 Elsevier B.V. All rights reserved.

1. Introduction

Dielectrics with high permittivity (the so-called high-k dielectrics) such as hafnium oxide HfO_2 (κ=12–40), zirconium oxide ZrO_2 (κ=12–40), aluminum oxide Al_2O_3 (κ=10) and some others are replacing traditional dielectrics in silicon devices: silicon oxide SiO_2 (k=3.9) and silicon nitride Si_3N_4 (κ=3.9) [1–3]. Recently, among all high-k dielectrics hafnia-based materials are considered as one of the most promising candidates for gate dielectrics in complementary metal-oxide-semiconductor (CMOS) technology, DRAM (dynamic random access memory) capacitors, and blocking insulators in Si-oxide-nitride-oxide-silicon (SONOS) – type flash memory cells [4,5]. Moreover, hafnium oxide shows interesting physical and chemical properties. It is widely used in optical fields because of its high refractive index, high optical transparency in the ultraviolet–infrared spectral range, and wide optical band gap (E_g=5.8–6.2 eV) [6–9].

One of the main problems on the way of HfO_2 mass implementation in the technological process is high conductivity caused by defects in high concentration. Oxygen vacancies are the most probable and spread defects responsible for high conductivity. Thus, the identification of oxygen vacancies in HfO_2 and their concentration control are important tasks [10–15]. Such control can be effectively performed by using the luminescent methods. In low-temperature photoluminescence (PL) spectra of HfO_2 crystals or films the emission band of defects can be detected in the region of 2.7–3.1 eV [13–15]. An UV intrinsic emission band of self-trapped excitons (STE) was observed in the region of 4.4 eV [7,8,9]. Pure HfO_2, however, becomes crystalline at temperatures lower than 500 °C. For high-k gate dielectrics, an amorphous structure is always preferred because a polycrystalline film can introduce high leakage paths along grain boundaries. Hafnium aluminate has been proposed as an alternative material, as it is a good barrier against oxygen diffusion, and it remains amorphous at relatively high temperatures.

* Corresponding author. Tel.: +7 343375 4711; fax: +7 343374 3884.
E-mail address: vpustovarov@bk.ru (V.A. Pustovarov).

http://dx.doi.org/10.1016/j.jlumin.2015.10.053
0022-2313/© 2015 Elsevier B.V. All rights reserved.

On the other hand, the exceptional properties of alumina (Al_2O_3), such as great hardness, high thermal and chemical stability, and high melting temperature, make it a very attractive material. The crystalline α-Al_2O_3 phase (corundum or sapphire) is the only stable modification of alumina. Crystalline α-Al_2O_3 has a band gap E_g=9.2–9.4 eV [16,17] and is widely used in optical devices. Sapphire doped with chrome (ruby) or titanium is applied as an active medium in laser techniques. Alumina is a highly radiation-resistant material and it is widely used as a high sensitive detector of ionizing radiation in dosimetry applications. The formation of defects in irradiated α-Al_2O_3 is the subject of numerous researches [16–22]. It should be noted that similar to both single crystal and films of HfO_2, STE emission was also observed in α-Al_2O_3 crystals. However, a high-energy emission band of A-type STE (7.6 eV) lies in the vacuum ultraviolet (VUV) range [17]. The detection of this VUV emission introduces the well-known experimental requirements and is not a trivial task.

It is well known that photoluminescence spectroscopy is among the most effective non-destructive methods for the study of defects in wide gap dielectrics. In this paper, we use PL method in the wide VIS–UV–VUV energy ranges for investigation of radiative phenomena due to defects and STE emission in the films of $Al_xHf_yO_{1-x-y}$ solid solutions. At the minimum value of x=0 we revealed the emission band of STE in pure HfO_2 film (4.4 eV) and at the minimum value of y=0 we revealed the emission band of STE in pure α-Al_2O_3 film (7.74 eV) in the VUV range. At the same time, the variation of the values of x enables control of the relative concentration of anion vacancies and their influence on the yield of STE emission in HfO_2 and α-Al_2O_3 films.

2. Experimental details and objects

2.1. Photoluminescence measurements

The present study was carried out by means of the low-temperature time-resolved luminescence spectroscopy in VUV. We applied selective excitation of the studied films in the soft X-ray region using synchrotron radiation (SR) from BW3 channel (HASYLAB, DESY, Hamburg) at the special setup developed for luminescence investigations [23]. Time-resolved photoluminescence (PL) spectra in VIS–UV–VUV regions (2.5–9.5 eV) as well as PL decay kinetics for the above mentioned crystals at T=7.2–8.0 K were measured. The PL spectra were registered by a 0.4 m vacuum monochromator (Seya–Namioka scheme) equipped with a microchannel plate-photomultiplier (MCP1645 Hamamatsu). To measure the temporal structure of the PL spectra, we used registration in two independent time windows Δt with the span Δt_1=5.7 (fast component) and Δt_2=21 ns (slow component), and the delay after excitation SR-pulse equal to δt_1=0.1 ns and δt_2=16 ns, respectively. The effective temporal resolution of the whole detection system was about 0.5 ns.

Under VUV excitation, the time-resolved PL spectra, PL decay kinetics and PL excitation spectra were measured on a SUPERLUMI station (channel I, HASYLAB, DESY) [24]. The measurements of the PL spectra were carried out using an ARC Spectra Pro-308i monochromator and R6358P Hamamatsu photomultiplier tube. The PL spectra were recorded in two time windows – fast: delay δt_1=0.6 ns, span of time windows Δt_1=2.3 ns; – slow: δt_2=58 ns, Δt_2=14 ns. The time resolution of the entire detection system was 1 ns (FWHM). The temporary interval between excitation SR pulses was 96 ns. The PL excitation spectra were corrected to an equal number of photons incident on the sample recorded with the use of sodium salicylate.

2.2. Films preparation

The objects of study were films of $Al_xHf_yO_{1-x-y}$ solid solutions with x=0; 4; 17; 20 at%. $Al_xHf_yO_{1-x-y}$ films were grown in a flow-type chemical vapor deposition (CVD) reactor using $Al(acac)_3$ (acac=pentane-2,4-dionate) and $Hf(thd)_4$ (2.2.6.6 tetramethyl-3.5 hafnium heptandionate) as precursors and argon as a carrier gas. $Al_xHf_yO_{1-x-y}$ thin films with various concentrations of Al, homogeneous and nonhomogeneous distributions of elements along the films thickness were purposefully grown by CVD. In addition, the atomic layer deposition (ALD) method was used to prepare pure Al_2O_3 films. $Al(CH_3)_3$ was used as a precursor. $Al_xHf_yO_{1-x-y}$ films were deposited on n-type Si (100) substrates at the temperature of 650 °C. Si substrates were treated by a sequence of chemical cleaning in CCL_4, and acetone. Etching was carried out in the H_2SO_4:HNO_3=1:1 mixture, and for final etching the diluted HF (50%) solution was used. The cleaning procedure resulted in removal of the native oxide and surface contaminations. The experimental setup and techniques were described in detail elsewhere [25].

The structure of the films was studied by X-ray diffraction (XRD) measurements at the station “Anomalous scattering” in the Siberian Center of Synchrotron Radiation (Institute of Nuclear Physics SB RAS, Novosibirsk, Russia). The chemical composition of films and its changes along the films thickness were studied with X-ray photoelectron spectroscopy (XPS) on a VG ESCALAB HP spectrometer using non-monochromatic Al Kα radiation. The film thickness (d) and refractive index (n) were measured with a single wavelength LEF-3M ellipsometer equipped with a He–Ne laser (λ=632.8 nm).

Description of relevant properties of the studied samples is presented in Table 1. However, we should introduce some explanations here. Our research presented in Section 3.1 below has shown that the films are the ones of solid solutions in which Hf^{4+} is replaced by aliovalent Al^{3+} impurity. As a result, oxygen vacancies are formed for local compensation of charges. Therefore, in order to show that the film is not a stoichiometric mixture of the two oxides, but a solid solution, we use chemical formula $Al_xHf_yO_{1-x-y}$. The values of x and Al/Hf ratio were determined from XPS data. Accordingly, we indicated the concentration of oxygen in this formula in Table. 1. Determining the concentration of oxygen vacancies in the studied films of solid solutions is almost an impossible task for us as oxygen vacancies can form complexes and, moreover, they can have different charge states.

3. Experimental results

3.1. The films characterization

XPS revealed that the films consisted of aluminum, hafnium and oxygen atoms as expected. The films are solid solutions (alloys) with varying cation content of x. This follows from XRD and XPS data shown in Figs. 1 and 2. Fig. 1 demonstrates a comparison of the films diffraction patterns with different aluminum

Table 1
The properties of films studied.

Film type	x (at%)	Al/Hf ratio	d (nm)	n
m-HfO_2	0	0	94	2.12
$Al_{0.04}Hf_{0.4}O_{0.56}$	4	0.1	139	1.84
$Al_{0.17}Hf_{0.28}O_{0.55}$	17	0.6	140	1.8
$Al_{0.2}Hf_{0.22}O_{0.58}$	20	0.9	198	1.8
Al_2O_3 (ALD)			50	1.7
Al_2O_3 (CVD)			132	1.7

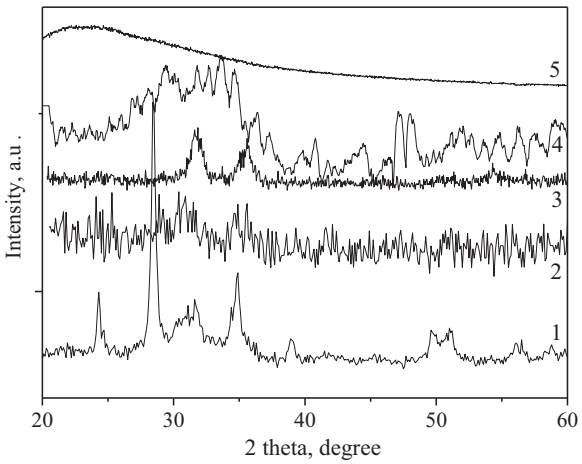

Fig. 1. Comparison of the film diffraction patterns: HfO_2 (1), $Al_xHf_yO_{1-x-y}$ (2–4), $x=4$, 17, 20 at%, respectively and Al_2O_3 film prepared by ALD methods according to Ref. [22] (5).

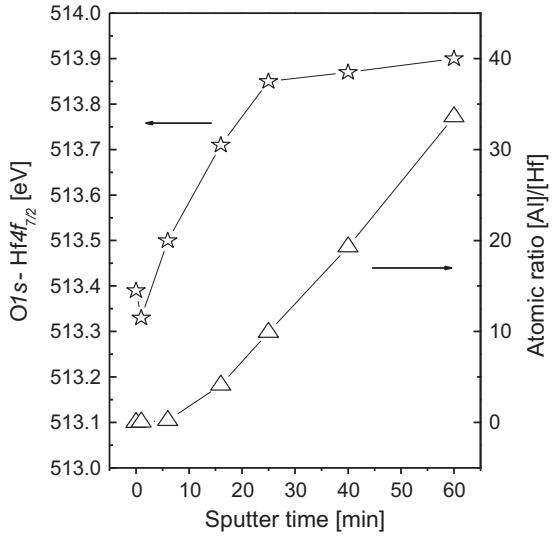

Fig. 2. The dependences of the O 1s and Hf $4f_{7/2}$ binding energy difference and the atomic ratio of Al/Hf on the time etching of the sample by Ar ions.

contents. Spectra of the films with 4 and 17 at% are different from the pure monoclinic modification of HfO_2 (m-HfO_2). The reflexes in the diffraction patterns gradually shift to a greater 2θ values as Al concentration increases. As pointed in [26], the observed systematic shift of the peak position indicates the formation of solid solutions. The formation of solid solutions in the Al–Hf–O system was also confirmed by XPS analysis of the films with purposefully grown gradient distribution of Hf and Al along the films thickness (Fig. 2). During analysis, the photoelectron spectra of the Hf 4f and Al 2p core levels were recorded at various etching times using Ar ion sputtering. It was found that increasing Al/Hf ratio was accompanied with the increase by O 1s and Hf $4f_{7/2}$ binding energy differences (Fig. 2). This relationship also confirms the formation of the solid solutions rather than a mixture of HfO_2 and Al_2O_3 separated phases. The local structure of Hf in $Al_xHf_yO_{1-x-y}$ amorphous films on silicon with uniform distribution of Al along the film thickness was studied by Extended X-ray Absorption Fine Spectroscopy (EXAFS) [25].

Thus, the use of XRD, XPS and EXAFS techniques allowed us to conclude that a continuous number of solid solutions occur in the films obtained by co-deposition from vapors of complex compounds of aluminum and hafnium.

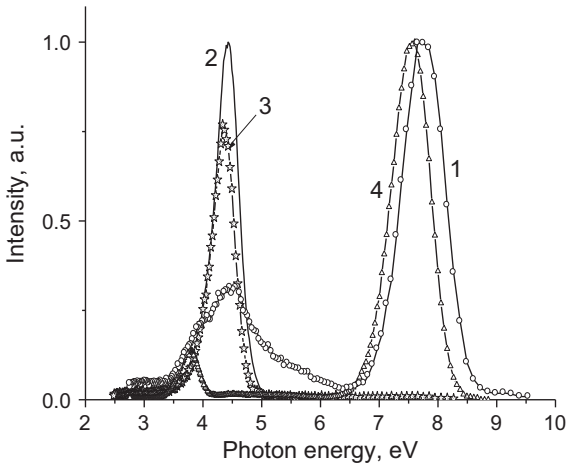

Fig. 3. Time-integrated PL spectra of the films: Al_2O_3 (1), HfO_2 (2), $Al_xHf_yO_{1-x-y}$ with $x=17$ at% (3) and α-Al_2O_3 single crystal (4) under $E_{exc}=130$ eV at $T=7.2$ K. The curve (1) shows the PL spectrum measured in the film prepared by ALD method.

X-ray diffraction patterns of Al_2O_3 films obtained by ALD are presented in Ref. [22]. We give these data from Ref. [22] in Fig. 1. XRD analysis shows that deposited films were amorphous. The films were crystallized after 2 h annealing in vacuum at the temperature of 900 °C: the diffraction lines appeared in X-ray diffraction patterns [22].

3.2. Soft X-ray excitation

Photons with energy $E_{exc}=130$ eV were used for PL excitation. First, this energy corresponds to the maximum photon flux provided by the BW3 beamline. Second, this energy is higher than the binding energy of L_{1-3} levels of aluminum and O_{1-3} levels of hafnium. When the film thickness is 100 nm, the transmittance of thin film is 9% in HfO_2 ($\rho=9.68$ g/cm3) and 5% in Al_2O_3 ($\rho=3.97$ g/cm^3) at $E_{exc}=130$ eV. This calculation was performed using the methodology described in Ref. [27]. Thus, the photons with energy of 130 eV were almost completely absorbed in these films providing maximum excitation efficiency.

Fig. 3 shows PL spectra of the studied films with different contents of cations (x, at%). For a pure Al_2O_3 film the PL spectrum contains a high-energy emission band with the maximum at 7.74 eV (FWHM=0.84 eV), and the low-energy emission bands covering energy range 3.8–4.5 eV. It should be noted that curve 1 shows the PL spectrum measured for Al_2O_3 film prepared by the ALD method. This high-energy emission band is not detected in the films of solid solution as well as in Al_2O_3 film prepared by a CDV method. This fact indirectly indicates a relatively high concentration of defects in the film prepared by the CDV method and lack of symmetry of the crystal lattice required for self-trapped exciton (STE) formation. Further, for comparison, Fig. 3 also shows the PL spectrum of nominally pure α-Al_2O_3 single crystal at the same excitation energy. It contains emission bands with the maximum at 7.56 eV (FWHM=0.77 eV) and 3.8 eV. The maximum of high-energy emission band in the film is shifted to higher energies (the value of shift is 0.18 eV), and the FWHM of this band increases. Furthermore, the PL decay kinetics of this film is characterized by a shorter PL decay time, see comparison in Fig. 4. The presence of this high-energy emission band in the PL spectrum is consistent with the data of XRD analysis that shows the dominant content of α-phase in the annealed Al_2O_3 films. At the same time it should be noted that the submitted PL spectra do not contain emission bands characteristic for other γ- δ- and Θ-phases of Al_2O_3. The PL spectra of these phases in Al_2O_3 had been studied previously [28,29].

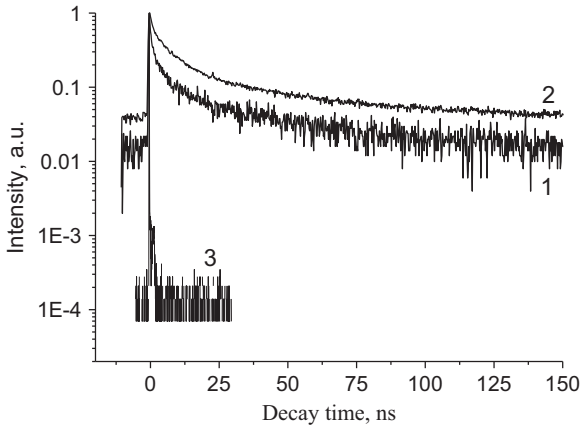

Fig. 4. PL decay kinetics of Al_2O_3 film (1) and α-Al_2O_3 single crystal (2) E_{exc}=130 eV, E_{emis}=7.6 eV, T=7.2 K. An approximation using two exponentials: τ_1=1.3 ns+τ_2=21 ns+long component (pedestal) 1.6% – (1); τ_1=3.3 ns+τ_2=27 ns+long component (pedestal) 4.4% – (2). The profile of the excitation pulse, measured by recording system (3).

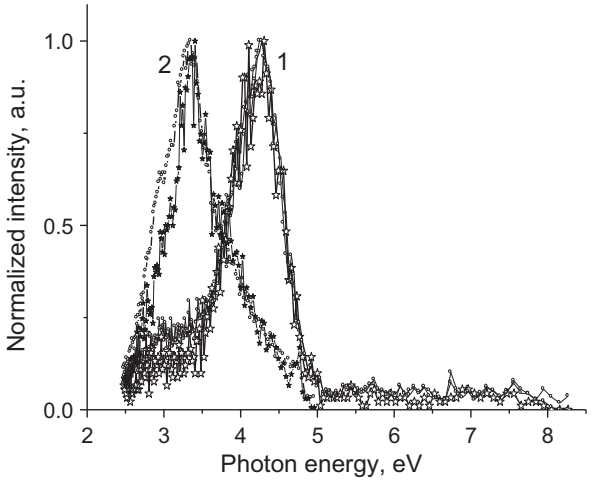

Fig. 5. Time-resolved PL spectra of $Al_xHf_yO_{1-x-y}$ films with x=4 (1) and x=20 at% (2) under E_{exc}=130 eV at T=7.2 K. Mugs – fast windows, stars – slow windows.

For a pure m-HfO_2 film the PL spectrum contains an emission band at 4.42 eV (FWHM=0.48 eV), Fig. 3. In pure monoclinic HfO_2 single crystals this band corresponds to radiation decay of STE [7,8,9]. The PL decay kinetics of UV emission in HfO_2 contains only slow components of ms–μs ranges. Therefore, only the time-integrated spectrum is shown in Fig. 3. This PL spectrum does not feature low-energy emission bands typical for defects [7], so in this case we do not observe luminescent manifestation of defects in hafnia.

In the films of solid solutions when the values of x=4, 17, 20 at%, the spectra and PL

decay kinetics vary considerably, see Figs. 3, 5 and 6. We can identify the following changes:

i) the high-energy emission band of 7.74 eV is completely quenched even when hafnium is introduced into solid solution independently of its concentration;

ii) if the values of x=4 and 17 at%, the maximum of 4.42 eV emission band shifts to 4.25 eV, the half-width increases (FWHM=0.80 eV), a short nanosecond component appears in the PL decay kinetics, Fig. 6;

iii) the 4.25 eV emission band is preserved in the PL spectra for the values of x=4 and x=17 at%;

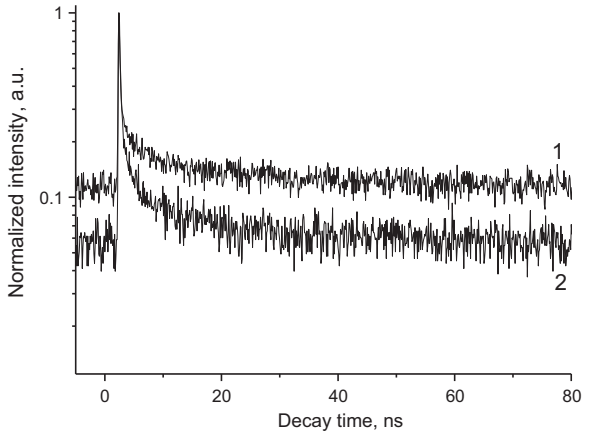

Fig. 6. PL decay kinetics of $Al_xHf_yO_{1-x-y}$ films with x=4 (1) and x=17 at% (2) E_{exc}=130 eV, E_{emis}=4.3 eV, T=7.2 K.

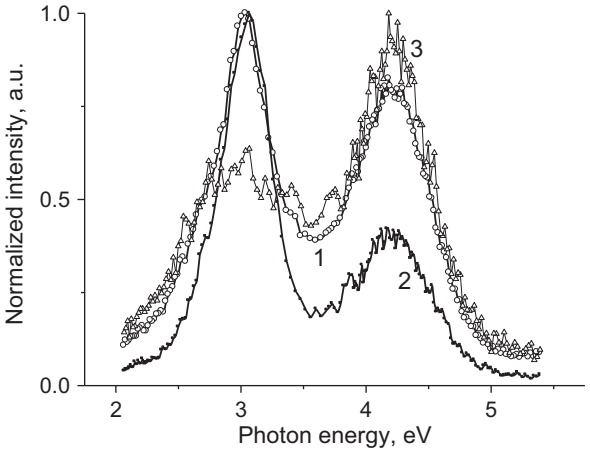

Fig. 7. Time-resolved PL spectra of $Al_xHf_yO_{1-x-y}$ films with x=4 at% under E_{exc}=5.96 eV at T=8 K: time-integrated (1), fast time windows (2) and slow time windows (3).

iv) when the x value increases from 4 to 20 at%, the intensity of low-energy emission bands in the region of 2.8–3.3 eV grows, Fig. 5;

v) when the value of x=20 at%, the time-resolved PL spectra show two low-energy emission bands with different PL decay kinetics. At the same time, the 4.25 eV emission band is almost quenched, Fig. 5.

It is noteworthy that changes in the spectral properties (peak position and FWHM) of STE luminescence have been observed in various phases of hafnia and zirconia [30]. The effect was assigned to the presence of various defects near STE, which varies spectral properties of the related luminescence bands.

3.3. Ultraviolet (UV) and vacuum ultraviolet (VUV) excitation

Time-resolved PL spectra under UV–VUV excitation are presented in Fig. 7. Like under soft X-ray excitation, these PL spectra contain a high-energy emission band at 4.22–4.42 eV and a non-elementary broad emission band in the region of 2.8–3.2 eV. If the value of x=0 (it is a pure m-HfO_2 film), the broad band at 4.42 eV with microsecond PL decay kinetics dominates brightly in the PL spectrum. In the films of solid solution the intensity of the low-energy bands grows with increasing x value. At the same time, the maximum of high-energy emission band shifts from 4.42 to 4.22 eV and the band intensity decreases with increasing x value. In addition, the fast ns-component appears in the 4.22 eV PL decay

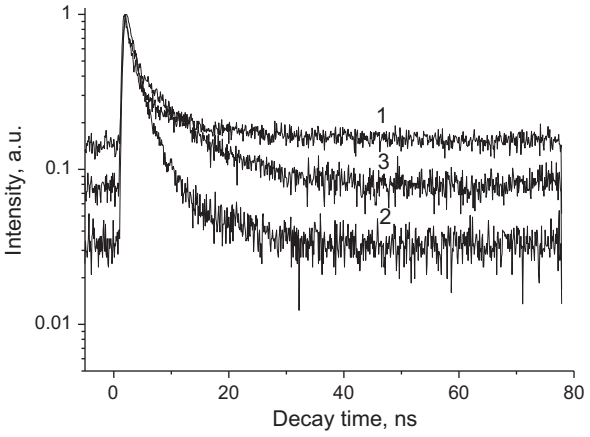

Fig. 8. PL decay kinetics of $Al_xHf_yO_{1-x-y}$ films with $x=4$ (1, 3) and 20 (2) at% under $E_{exc}=5.96$ eV at $T=8.0$ K: $E_{emis}=4.26$ (1,2) and 3.1 eV (3).

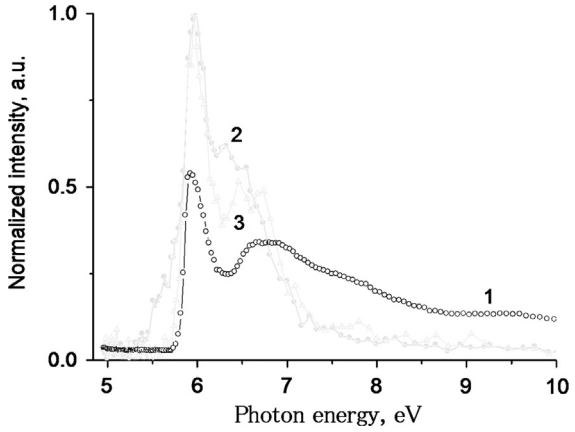

Fig. 9. Time-resolved PL excitation spectra of HfO_2 (1) and $Al_xHf_yO_{1-x-y}$ with $x=4$ at% (2) films: $E_{emis}=4.3$ eV, $T=8.0$ K.

kinetics. As an example, the PL spectra are shown in Fig. 7 when the value of $x=4$ at%. Moreover, Fig. 8 shows the PL decay kinetics measured for different low-energy emission bands. It should be noted that the PL decay kinetics contains this nanosecond component even if the concentration of aluminum increases up to $x=20$ at% (curve 3).

The PL excitation spectra for different emission bands in $Al_xHf_yO_{1-x-y}$ films are shown in Figs. 9 and 10. The time-integrated spectrum and the spectrum of the slow component show that the 4.22 eV emission band excited only by photons with energies $E_{exc} > 5.8$ eV (the maximum is at energy of 5.96 eV) are in agreement with the data presented in Ref. [7] for HfO_2 films. At the same time, the fast component of the PL decay kinetics is excited also in the low energy region of 5.5 eV. This energy corresponds to the fundamental absorption edge in HfO_2, Fig. 9. The time-resolved PL excitation spectra for 3.1 eV emission band differ more significantly. As an example, these spectra are shown in Fig. 10 when the value of $x=4$ at%. It should be noted that the spectrum measured in the fast time windows contains a weak peak at energy of 4.1 eV and dominant bands with maxima at energies of 5.25 eV and 6.1 eV. The first two bands are located in the energy gap, which allows us to assign them to the defect states.

4. Discussion of experimental results

In nominally pure α-Al_2O_3 single crystals ($E_g=9.2$–9.4 eV) the low temperature PL spectra contain the emission bands at 7.6 and

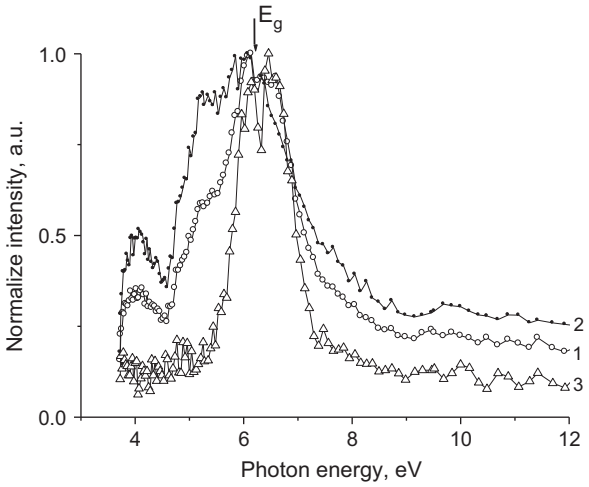

Fig. 10. Time-resolved PL excitation spectra of $Al_xHf_yO_{1-x-y}$ films with $x=4$ at%: $E_{emis}=3.1$ eV, $T=8.0$ K, time-integrated (1), fast time windows (2) and slow time windows (3). The arrow shows the band gap energy position in HfO_2 single crystals according to Refs. [6–8].

3.8 eV, which are attributed to the emission of self-trapped excitons (STE) of A- and E-type, respectively [17,19,23]. In single crystals with intentionally induced defects, the PL spectra feature strong emission bands of F^+ centers (maximum is at 3.8 eV) and F centers (maximum is at 3.0 eV) [16,18–21]. In addition, some authors observed the emission band in the region of 4.2–4.4 eV associated with uncontrolled impurities or defects of crystalline structure [31]. Therefore, the low-energy bands in the PL spectrum of Al_2O_3 film (Fig. 3, curve 1) are logically associated with PL defects or impurity centers.

According to Ref. [23], in α-Al_2O_3 single crystals the intrinsic 7.6 eV. A emission band can be effectively excited at the direct photocreation of excitons by photons with energy ~8.85–9.1 eV at the fundamental absorption edge or with the recombination of free electrons and free holes. These exciton states are interpreted as radiative decay of self-shrunk excitons. Self-shrunk excitons are a kind of STE. This term was proposed in Sumi theory [35]. This theory considers various STE states in the acustic phonon field. Even if electron–phonon or hole–phonon interactions alone are insufficient for an electron or hole to transfer to the self-trapped state, an exciton as a whole may still become self-trapped when the deformations generated by an electron and hole are summed. Exactly such exciton states were termed self-shrunk excitons. They are effectively excited in the region of the long wavelength fundamental absorption edge and they are observed in some oxide crystals [23].

Long-term studies of α-Al_2O_3 crystals did not lead to the detection of immobile self-trapped holes or electrons. However, the theoretical model of Sumi allows the existence of such immobile self-shrunk excitons even if an electron and a hole do not separately undergo self-trapping. In α-Al_2O_3 crystals the fast (τ ~6 and 20 ns) and slow (τ ~150 ns) components of PL decay kinetics of the A emission under VUV excitation correspond to the creation of singlet and triplet p^5s excitons [23].

In the studied α-Al_2O_3 film the maximum of a high-energy band (7.74 eV) in the PL spectrum shifts relative to the maximum of PL spectrum in the single crystal (7.6 eV). This emission band is wider (FWHM=0.81 eV) and they are characterized by shorter nanosecond PL decay kinetics, see Fig. 4. On the basis of these data, we believe that in the studied Al_2O_3 film the electronic states of STE are modified by defects and the so-called bound STE can be formed. This is possible if one of the charge carriers is localized on the defect, because their concentration is sufficient in the film

under study. Impurity-bound excitons [17,32,33] or defect-bound excitons (in this context, these defects are F-like centers) [18,19] have emission bands with a large Stokes shift. They were observed in α-Al_2O_3 single crystals earlier. However, the modification of the electron states of A-type STE with an emission band in the VUV region, as far as we know, is observed in α-Al_2O_3 for the first time. However, it should be noted that at present we do not exclude the influence of the surface on the PL spectrum in this thin film since its thickness is only 50 nm.

In pure single crystals and films of monoclinic HfO_2 (E_g=6.2 eV) the low temperature PL spectra contain a 4.4 eV emission band with slow microsecond PL decay kinetics. This PL band is attributed to emission of STE [8,9]. The PL spectrum shown in Fig. 3 (curve 2) confirms this result. It is known that in HfO_2 crystals with defects the PL spectra contain the low-energy luminescence bands the region of 2.8–3.1 eV, at the same time in such crystals the STE emission is quenched and this STE band is not detected in PL spectra [14,15].

$Al_xHf_yO_{1-x-y}$ films can be viewed as a matrix of HfO_2 with varying concentrations of defects when the value of x changes. The point defects are formed in the anion sublattice of HfO_2 as compensators of the local charge. Consequently, the concentration of anion vacancies in hafnium oxide increases with an increasing value of x. In the studied films of solid solutions when the value of x=4 or 17 at%, the maximum of STE luminescence band shifts to lower energies (the shift is 0.18 eV), the value of FWHM increases (Figs. 5 and 7), a short nanosecond component (τ=2.4 ns) appears in the PL decay kinetics (Figs. 6 and 8), which is in agreement with the results in Ref. [30]. This short ns-component in the PL decay kinetics is preserved when aluminum concentration is increased up to the value of x=20 at% (Fig. 8, curve 3). In addition, the PL excitation spectrum measured with a time resolution (the spectrum measured in fast time windows, Fig. 9, curve 2) contains singularity in the region of 5.5 eV (below the fundamental absorption edge in HfO_2). When the value of x=20 at%, the STE emission band is practically quenched, only low-energy bands are observed in the PL spectrum. However, in contrast to the PL excitation in the soft X-ray region (in this case band charge carriers with high kinetic energy are created) the STE luminescence under VUV excitation is observed even at the value of x=20 at%.

The revealed changes can be interpreted as a manifestation of excitons bound on defects in the studied films of solid solutions. Indeed, the presence of defects perturbs the energy of STE excited state, accordingly, the efficiency of energy transfer to the defects is changed. When the value of x=4, 17, 20 at%, the low-energy broad luminescence bands in the PL spectrum of $Al_xHf_yO_{1-x-y}$ films (Figs. 5 and 7) correspond to the emission of defects in hafnium oxide. The 2.8 eV emission band is associated with oxygen vacancies. The nature of a band at energies above 3 eV is not yet established [10–15,34]. According to these papers, the PL excitation spectrum of this 2.8 eV band contains a selective maximum at the energy of 5.2 eV. Indeed, the PL excitation spectrum contains selective bands at the energies of 4.1 and 5.25 eV (Fig. 10, curve 2). These bands are located in the region of transparency of hafnium oxide. This fact clearly shows the connection of these bands with the PL defects. In principle, these PL results are consistent with XRD analysis data (see Section 3.1), which shows amorphisation of films, when Al concentration is increased. Indeed, the PL emission bands in the low-energy region of 2.8 eV are typical for amorphous HfO_x films [14,15,34]. Moreover, the 2.8 eV PL excitation spectrum also contains a band in the region of 5.2–5.4 eV [14,15].

It should be noted that the PL defects were efficiently excited by photons with energies of $E_{exc} \geq E_g$, which can indicate energy transfer to the luminescence centers by charge carriers created in the conduction band. On the other hand, at high concentrations of Al (even when the value of x=4 at%), the emission band in the region of 3 eV may belong to F-centers in the matrix α-Al_2O_3. Absorption spectrum of these F-centers contains an intensity band (consequently, the band in the PL excitation spectrum) in the region of 5.9–6.2 eV [16,18]. However, the study of charge carrier transport in the films of solid solutions requires a separate detailed consideration in the future.

Thus, the increase of the x value (the increase of aluminum concentration and, accordingly, the increase of the concentration of anionic vacancies in solid solutions on base of HfO_2), on the one hand, leads to a drop in the yield of STE ultraviolet luminescence in hafnium oxide. On the other hand, the PL intensity of defects grows. These defects form broad bands with a significant Stokes shift in the PL spectra.

5. Conclusion

The PL of $Al_xHf_yO_{1-x-y}$ films obtained by CVD from separated sources of volatile complex organometallic compounds of Al and Hf was studied. The formation of solid solutions was confirmed by XRD and XPS measurements.

Applying soft X-ray and VUV excitation, the low-temperature time-resolved PL in $Al_xHf_yO_{1-x-y}$ films with different concentrations of aluminum (and respectively of anion vacancies) was studied. The revealed PL emission bands present in wide spectral VIS–UV–VUV ranges. Depending on the cation content (a value of x) in the PL spectra one can detect: i) the intrinsic luminescence of monoclinic HfO_2; ii) the intrinsic VUV-luminescence of α-Al_2O_3; iii) the luminescence of defects. The following results were obtained in our work.

In α-Al_2O_3 films prepared by ALD methods, the low temperature intrinsic luminescence of A-type STE is observed in the VUV-region (7.74 eV emission band, fast nanosecond decay time). In comparison with the PL of a single crystal, we assigned revealed luminescence bands in these films to the electronic states of STE modified by presence of the defects. The STE associated with defects can be formed. However, we cannot completely exclude the influence of the surface effects on the PL spectrum of thin films.

In $Al_xHf_yO_{1-x-y}$ films when the value of x=0 (HfO_2), the PL spectra contain a 4.4 eV emission band, which is associated with the STE emission in monoclinic HfO_2. In $Al_xHf_yO_{1-x-y}$ films when the value of $x > 0$, the STE emission band is modified, we observed photoluminescence of bound excitons on defects. The STE luminescence is quenched with increasing aluminum concentration (increase of the value of x), while the intensity of luminescence increases due to defects.

The low-energy emission bands in the PL spectra of $Al_xHf_yO_{1-x-y}$ films (when the value of $x > 0$) were ascribed to luminescence of defects (anion vacancies) in the crystalline structure of monoclinic HfO_2.

Thus, the results show that emission properties and relaxation processes of electronic excitations strongly depend on a degree of film imperfection. The PL results under soft X-ray and VUV excitation are in good agreement. However, the probability of radiative relaxation of electronic excitations with participation of defects or through STE states depends on energy of exciting photons. The difference in the kinetic energy of free charge carriers leads to different relaxation channels of radiation relaxation. As a whole, the results show that the time-resolved luminescent spectroscopy is a sensitive method to detect point defects and relax exciton states in these oxide films.

Acknowledgments

This work was partly supported by the Russian Science Foundation (Grant no. 14-19-00192), the Center of Excellence "Radiation and Nuclear Technologies" (Competitiveness Enhancement Program of Ural Federal University, Russia), HASYLAB DESY (Projects nos. 20110843, 20080119EC), Estonian Materials Technology Program (Project 3.2.1101.12-0014) and institutional research funding (IUT 2-26) of the Estonian Ministry of Education and Research.

References

[1] J. Robertson, R.M. Wallace, Mater. Sci. Eng. R 88 (2015) 1.
[2] T.V. Perevalov, V.A. Gritsenko, Phys. Uspekhi 53 (2010) 561.
[3] C. Zhao, C.Z. Zhao, S. Taylor, P.R. Chalker, Materials 7 (2014) 5117.
[4] G.D. Wilk, R.M. Wallace, J.M. Anthony, J. Appl. Phys. 87 (2000) 484.
[5] J.H. Choi, Y. Mao, J.P. Chang, Mater.Sci. Eng. 72 (2011) 97.
[6] T. Nishide, S. Honda, M. Matsuura, M. Ide, Thin Solid Films 371 (2000) 61.
[7] J. Aarik, H. Mandar, M. Kirm, L. Pung, Thin Solid Films 466 (2004) 41.
[8] M. Kirm, J. Aarik, M. Jurgens, I. Sildos, Nucl. Instrum. Methods A 537 (2005) 251.
[9] V. Kiisk, S. Lange, K. Utt, T. Tatte, H. Mandar, I. Sildos, Physica B 405 (2010) 758.
[10] L. Vandelli, A. Padovani, L. Larcher, R.G. Southwick, B. Knowlton, G. Bersuker, IEEE Trans. Electron Devices 58 (2011) 2878.
[11] D.M. Ramo, A.L. Shluger, J.L. Gavartin, G. Bersuker, Phys. Rev. B 99 (2007) 155504.
[12] S. Guha, V. Narayanan, Phys. Rev. Lett. 98 (2007) 196101.
[13] J.X. Zheng, G. Ceder, T. Maxisch, W.K. Chim, W.K. Choi, Phys. Rev. B 75 (2007) 104112.
[14] T. Ito, M. Maeda, K. Nakamura, H. Kato, Y. Ohki, Jpn. J. Appl. Phys. 97 (2005) 054104.
[15] T.V. Perevalov, V.Sh Aliev, V.A. Gritsenko, A.A. Saraev, V.V. Kaichev, E. V. Ivanova, M.V. Zamoryanskaya, Appl. Phys. Lett. 104 (2014) 071904.
[16] B.D. Evans, J. Nucl. Mater. 219 (1995) 202.
[17] M. Kirm, G. Zimmerer, E. Feldbach, A. Lushchik, Ch Lushchik, F. Savikhin, Phys. Rev. B Condens. Matter Mater. Phys. 60 (1999) 502.
[18] A.I. Surdo, V.S. Kortov, V.A. Pustovarov, Radiat. Meas. 33 (2001) 587.
[19] V.N. Makhov, A. Lushchik, Ch.B. Lushchik, M. Kirm, E. Vasil'chenko, S. Vielhauer, V.V. Harutunyan, E. Aleksanyan, Nucl. Instrum. Methods B 266 (2008) 2949.
[20] V.A. Pustovarov, V.Sh Aliev, T.V. Perevalov, V.A. Grizenko, A.P. Yelisseyev, J. Exp. Theor. Phys. 111 (2010) 989.
[21] T.V. Perevalov, O.E. Tereshenko, V.A. Gritsenko, V.A. Pustovarov, A.P. Yelisseyev, C. Park, J.H. Han, C. Lee, J. Appl. Phys. 108 (2010) 013501.
[22] V.A. Pustovarov, T.V. Perevalov, V.A. Gritsenko, T.P. Smirnova, A.P. Yelisseyev, Thin Solid Films 509 (2011) 6319.
[23] M. Kirm, A. Lushchik, Ch Lushchik, S. Vielhauer, G. Zimmerer, J. Lumin. 102–103 (2003) 307.
[24] G. Zimmerer, Radiat. Meas. 42 (2007) 859.
[25] T.P. Smirnova, L.V. Yakovkina, V.O. Borisov, V.N. Kichai, V.V. Kaichev,and, V. V. Kriventsov, J. Struct. Chem. 53 (2012) 718.
[26] L.V. Plyasova, Vvedenie v rentgenografiuy katalizatorov. Institute of Catalysis, Siberian Branch of RAS. Novosibirsk, 2010. (in Russian).
[27] ⟨http://henke.lbl.gov/optical_constants⟩.
[28] M. Kirm, E. Feldbach, A. Kotlov, P. Liblik, A. Lushchik, M. Oja, E. Palcevskis, Radiat. Meas. 45 (2010) 618.
[29] S.V. Gorbunov, A.F. Zatsepin, V.A. Pustovarov, S.O. Cholakh, V.Yu Yakovlev, Phys. Solid State 47 (2005) 733.
[30] M. Kirm, J. Aarik, E. Feldbach, S. Lange, H. Mandar, T. Uustare, Characterization of oxide thin films grown by atomic layer deposition using luminescence spectroscopy, in: K. Worhoff, D. Misra, P. Mascher, K. Sundaram, W.M. Yen, J. Capobianco (Eds.), Dielectrics in Emerging Technologies and Persistent Phosphor, 2005, pp. 133–140 , PV 2005-13.
[31] P.A. Kulis, M.J. Springis, A. Tale, J.A. Valbis, Phys. Status Solidi (A) 53 (1979) 113.
[32] V.A. Pustovarov, V.S. Kortov, S.V. Zvonarev, A.I. Medvedev, J. Lumin. 132 (2012) 2868.
[33] B.R. Namozov, V.A. Vetrov, S.M. Muradov, R.I. Zakharchenya, Phys. Solid State 44 (2002) 1459.
[34] E.V. Ivanova, M.V. Zamoryanskaya, V.A. Pustovarov, V.Sh Aliev, V.A. Gritsenko, A.P. Elisseyev, J. Exp. Theor. Phys. 147 (2015) 820.
[35] A. Sumi, J. Phys. Soc. Jpn. 43 (1977) 1286.